PHYS363: Astrophysics Laboratory

Solar Activity and the Solar Wind

Will Roscoe, Alex Wainman

January 2, 2025

Introduction

10:00 Solar phenomena originating from the Sun's surface and atmospheric layers impact Earth's environment. Incredibly hot plasma from the solar corona can generate solar wind which carries the interplanetary magnetic field (IMF) that influences the Earth. In this experiment, we aim to gain experience of handling data from various sources, to then understand dynamics and characteristics of solar phenomena such as the IMF and Solar Wind transients.

Part I Solar Activity and the Solar Cycle

10:02 We began by importing the data from the `sunspotnumbermonthly1749.txt` file and began formatting it correctly into QtiPlot so we could begin plotting. There was a lot of white space in the data that could be removed.

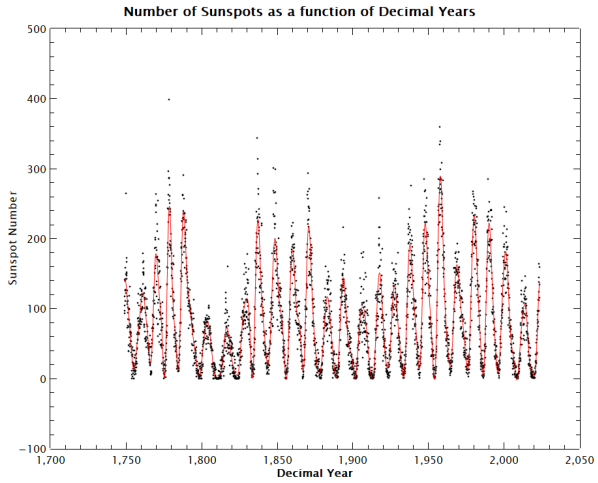

Figure 1: This figure shows the average monthly number of sunspots over the past 250 years. we can see that there are regular periods of higher and lower sunspots each month, suggesting that there is some cyclic behaviour.

10:24 Using the graph plotted we were able to estimate the average period of the solar cycle to be approximately 11.04 years by plotting a smoothing function. This also allowed us to see the variability in the number of sunspots with time as well. Although there are a large number of periods visible in the data, there is also an uncertainty visible due to many of the solar cycle periods having different lengths. As our answer doesn't demonstrate the variability in solar length we calculated the range of the periods to be able to estimate standard deviation which gave our answer to be (11.04 ± 0.65) decimal years.

10:43 The graph does demonstrate significant periods of 'long' minima in sunspot activity from approximately 1795 to 1825 as the more visible one, having a period of roughly 30 decimal years. This corresponds to the Dalton Minimum period which lasted from 1796 to 1820, having a period of 24 decimal years.

10:43 Similarly to the `sunspotnumbermonty1749.txt` data we formatted it so the data is approachable to begin plotting.

10:59 We plotted a graph of magnetic field strengths for both the North and South solar poles against time in decimal years to be able to observe the periodicity of the poles.

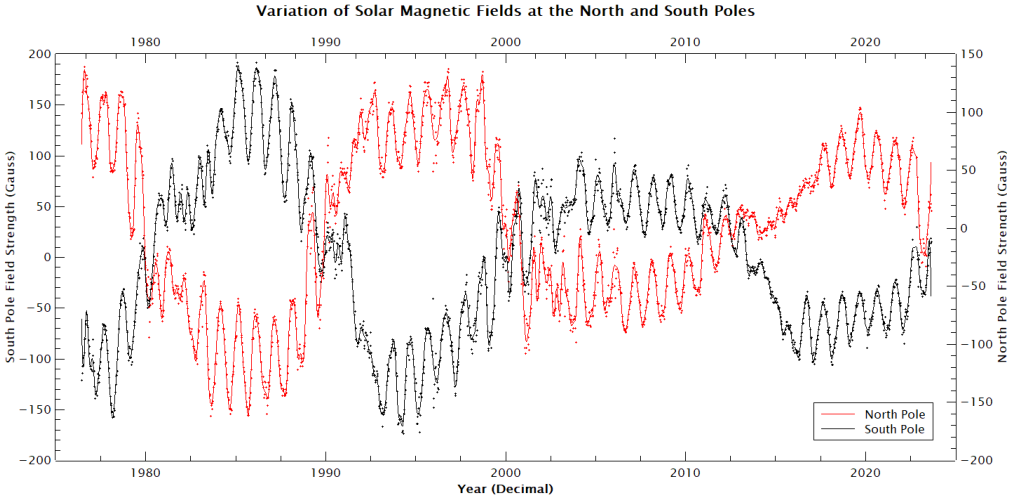

Figure 2: This plot shows the unfiltered signal from the poles data.

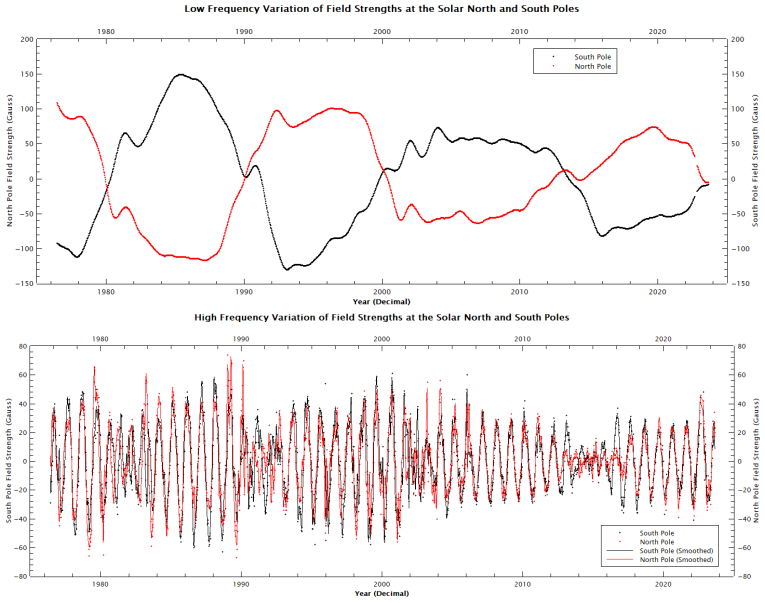

Figure 3: Low (Top Graph) and High (Bottom Graph) frequency variation of the poles. The high frequency variations were calculated by subtracting the Low frequency variation from the unfiltered data, found in Fig2. In the High frequency plot we can see that the North and South Pole field strengths have very similar cyclical trends. In the Low frequency variations we see the opposite, where maxima at the North Pole line up with minima at the south, and vice versa. The high frequency variation has a period ~ 1 yr, and the low frequency variation has a period 10-15 yrs.

11:24 We discussed the cause of the high frequency variation and concluded that it would likely be due to the orbital movement of the earth since the period matches the length of earths orbital period. This is also evidenced by the fact that it appears similarly across both North and South pole measurements. The data is affected by this since WSO is an earth based solar observatory.

11:33 By plotting the filtered polar field strength and sunspot number as a function of time, we are able to determine the average polar field strengths for the North and South poles at the solar maximums of the number of sunspots.

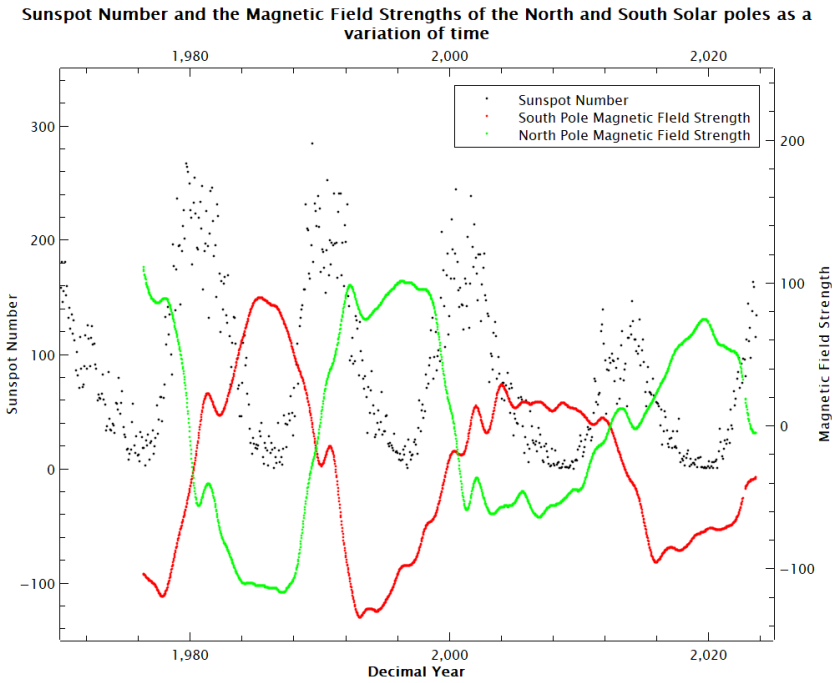

Figure 4: The North and South Pole Field Strengths have been plotted with the monthly average sunspot number for the period 1975-present. We see that the times of Solar Maxima (sunspot maxima) correspond to the times where North and South Pole field strengths are equal.

13:02 By using the plot it is clear that the average magnetic polar field strengths are close, to $0\mu T$. This is due to the reversal of the magnetic fields, during this time the fields become highly dynamic and disordered thus reducing their overall strength to zero before stabilising again.
In Figure 3 on the experiment guide, the left magnetogram demonstrates a more ordered structure with strong polar regions dominated by a singular polarity and thus indicates that it is the solar minimum. Therefore due to the more disordered field with mixed polarities across the surface, the right magnetogram is the solar maximum.
From this it is clear that the mechanism that produces sunspots is due to the sun's magnetic field dynamics. As shown in the right magnetogram of the solar maximum, the surface of the sun is highly disordered due to the magnetic field activity and as a result there is high amounts of flux out of the surface of the sun as a sunspot.

13:12 By using Fig4 we were able to estimate the periodicity of the magnetic fields to be approximately 22 years. Comparing this to the sunspot period of 11 years, it's clear that the magnetic field variation reflects a full cycle of polarity reversal.

Part II Interplanetary Space and the Solar Wind

13:15 We imported the data, omitting any entry containing “999” in (therefore excluding 9999.99 and 9999.99)

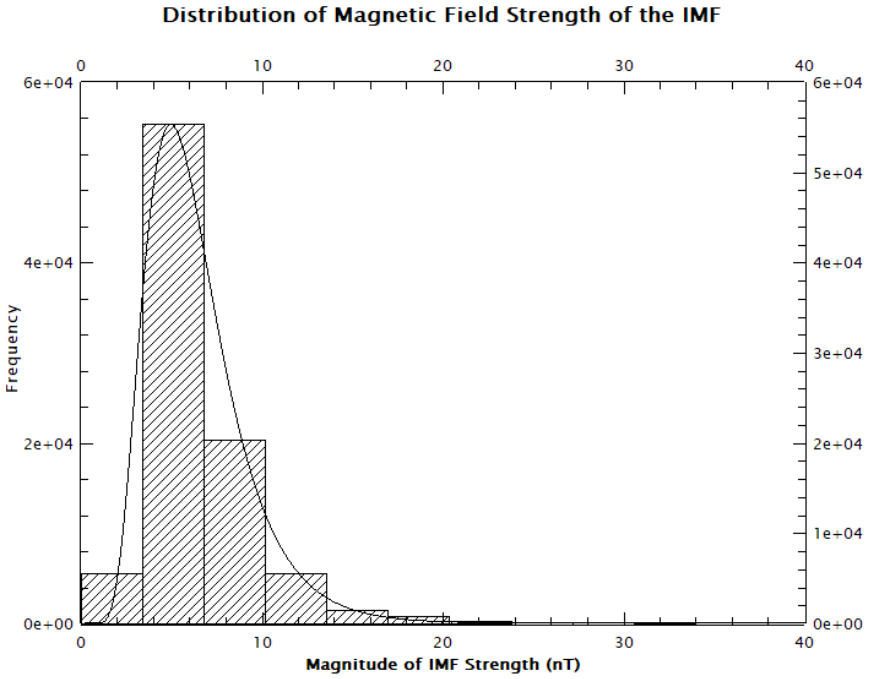

Figure 5: Histogram showing the distribution of magnitude of magnetic field strengths of the IMF with a 5 minute interval over 2022-23. There is a clear skewed normal distribution centered around 6nT , ranging from $1 \to 38$nT.

13:22 The generally agreed range of strengths is $1 - 37$nT, averaging around 6nT. This is in line with the distribution we found in Figure 5.
To calculate the expected field strength at $r_E = 1$AU, we will use the fact $\mathbf{B}(r) \propto r^{-2}$:

$$\mathbf{B}(r) \propto r^{-2} \begin{cases} B_E = K(r_E)^{-2} \\ B_s = K(R_\odot)^{-2} \end{cases} \implies B_E(r_E)^2 = K = B_s(R_\odot)^2$$

$$B_E = B_s \left(\frac{r_\odot}{R_E}\right)^2 = 0.2\ [\text{mT}] \cdot \left(\frac{696340\ [\text{km}]}{1.496 \cdot 10^8\ [\text{km}]}\right)^2 = 4.33\ \text{nT}$$

where B_s is the field strength at the surface of the sun, B_E is the field strength at Earth orbital radius, $r_\odot$ is the Sun’s radius and R_E is the Earth’s orbital radius.

13:34 from the `OMNI2_H0_MRG1MNTH.txt` data we plotted a graph of the magnitude of the IMF-B against time to see how it fluctuates and varies over time. After this we then superimposed the sunspot data on top to allow us to compare how the IMF-B varies as the number of sunspots varies.

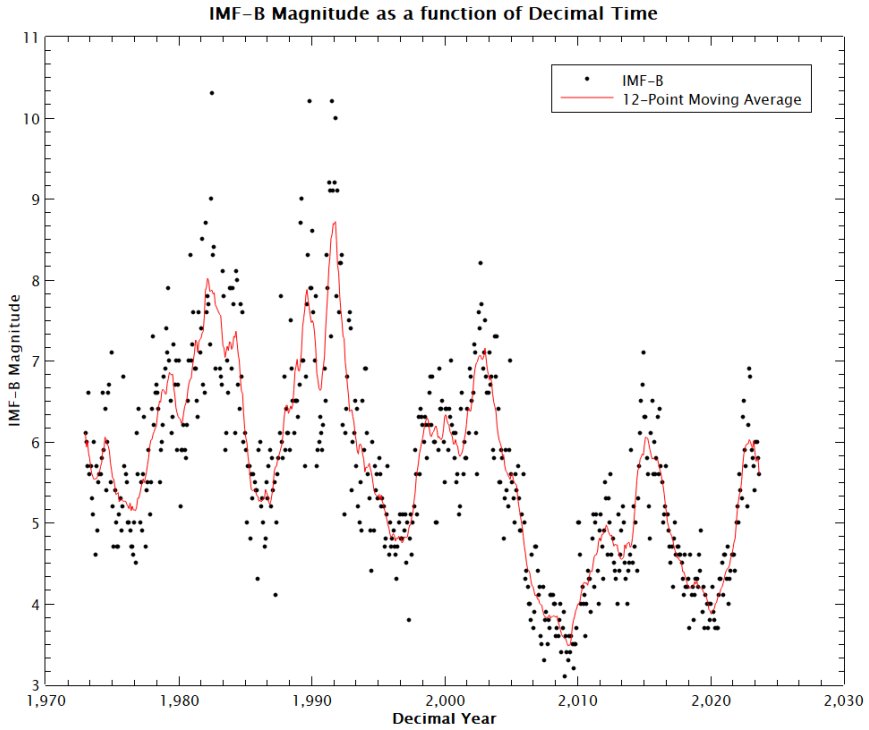

Figure 6: From the figure we can see how the IMF-B strength fluctuates and varies over time and has periods of minima and maxima.

13:49 By superimposing the sunspot data and taking a 12-point smoothing fit of it as well we were able to produce a graph that demonstrates how IMF strength varies with the solar cycle.

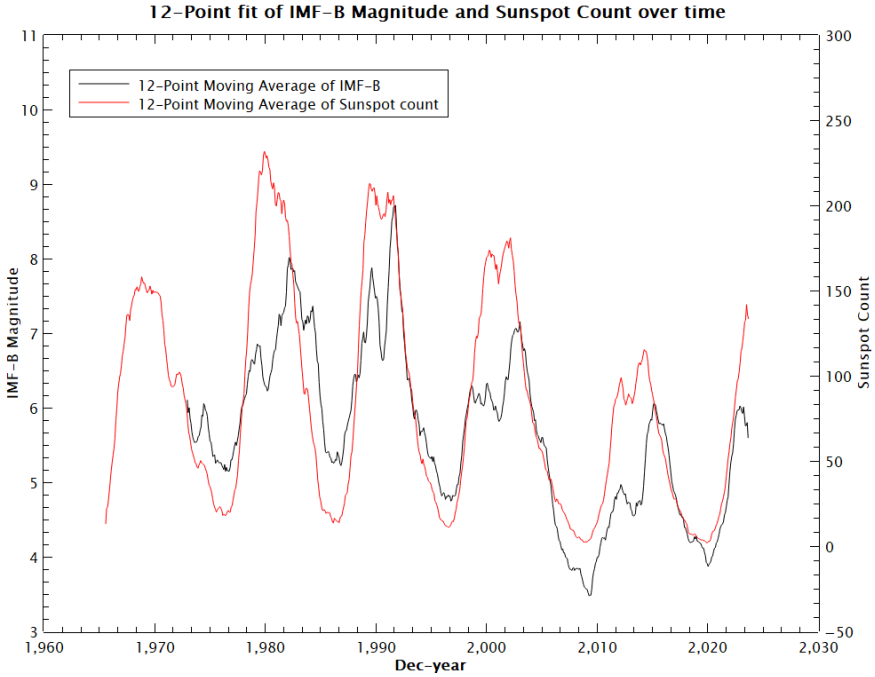

Figure 7: The graph shows how the IMF-B varies with the solar cycle. It is clear that the IMF Magnitude increases during the sunspot maximums occur as the poles reverse due to the increased flux through the surface of the sun during this period. The data points have been omitted so that the 12-Point moving averages can be seen more easily

14:01 We then moved on to plotting the solar wind speed as a function of time to give the graph for part 2.2(b).

14:07

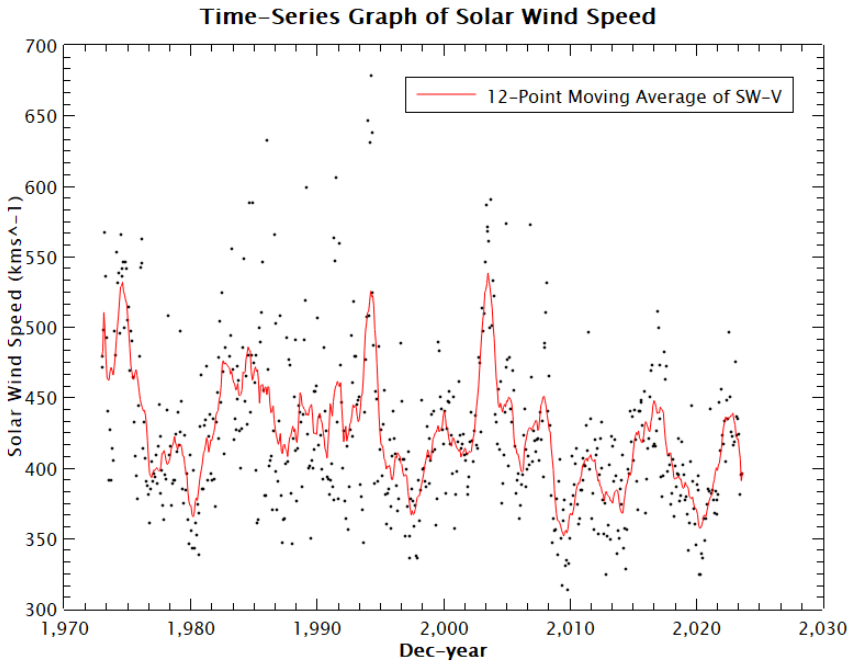

Figure 8: From the figure it is clear that the solar wind speed is following a similar pattern to the IMF-B strength and how it fluctuates and varies over time.

Having plotted this graph we moved on to superimposing the sunspot data like we did before with the IMF-B 12-point moving average.

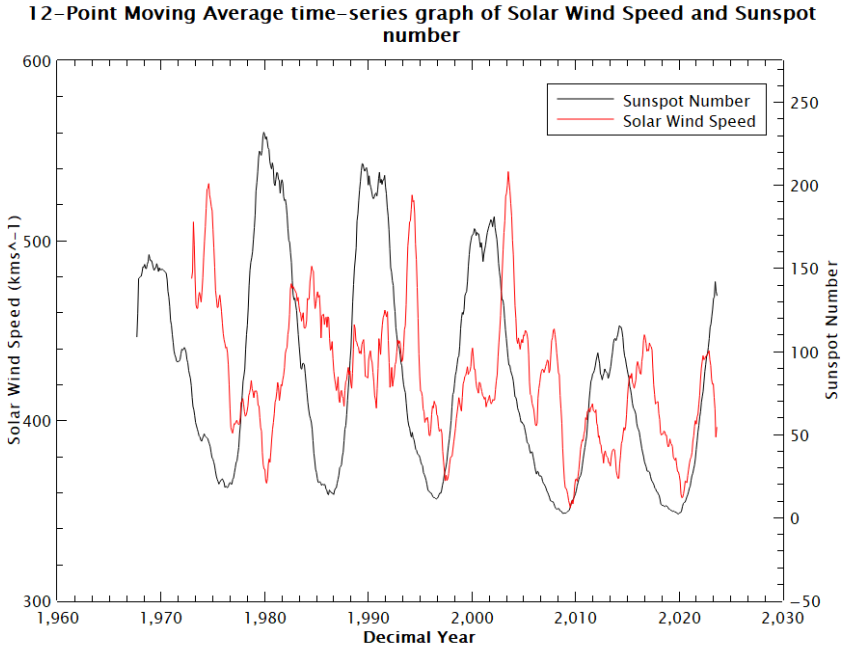

Figure 9: A 12-point moving average graph of solar wind speed and sunspot number. From the figure it is clear that the solar wind speed peaks are shifted to the right of the sunspot peaks, implying that the decay of sunspots leads to increased solar wind speed as flux and plasma are emitted from the surface of the sun

14:22

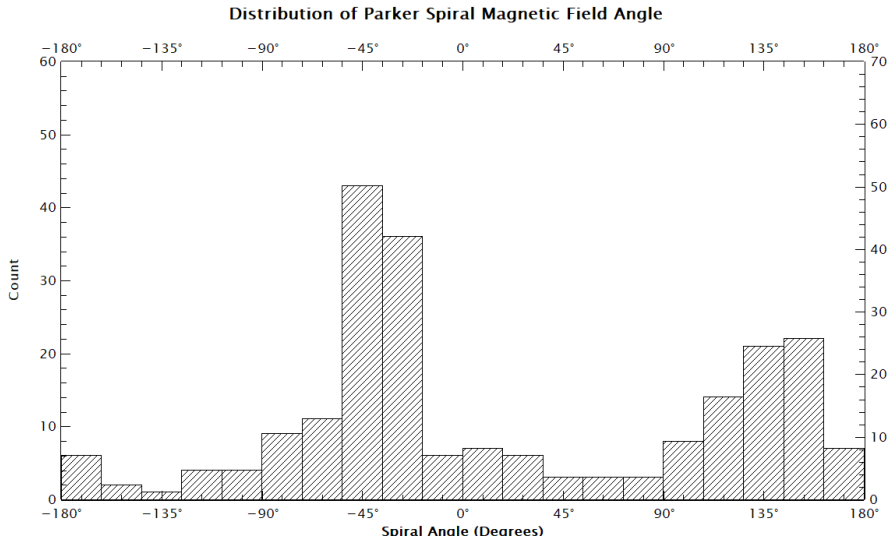

Figure 10: Histogram showing the distribution of angles of the Parker Spiral. There are two peaks around $-45°$ and $140°$, which are approximately opposite one another. This is in-line with our understanding of the IMF sheet, and the Parker Spiral having two maxima, due to the frozen-in theorem. The angle of $45°$ matches up with the expected value for near-earth observations.

14:35

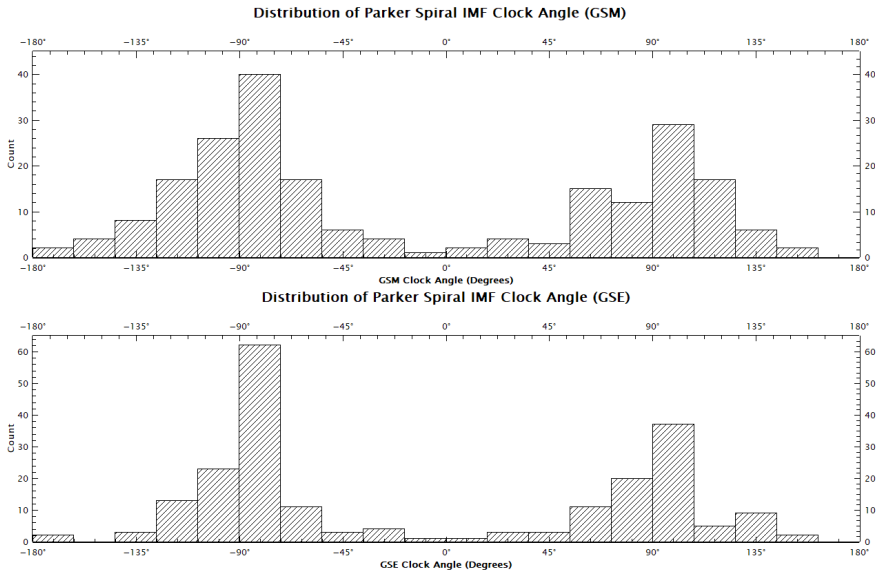

Figure 11: Histogram showing the clock angle of the IMF in Both GSE(left) and GSM(right) coordinate systems. On both graphs we see two clear peaks: for GSE and GSM systems at $\pm 90°$, with differing peak strengths.

The shape of the distributions found in Fig. 11 are consistent with expectations, where both show maximal frequency of clock angles around $\pm 90°$, corresponding to near zero $\mathbf{B}_z$ component. This is expected since the observations were made near-earth, where the IMF sheet has flattened out more in comparison to measurements made closer to the Sun.

Part III Solar Wind Transients

14:48 We calculated the days of the year by using the equation $\frac{Secs-of-year}{24*60^2} + 1$, giving us the time in days
14:52 to be able to plot a time-series graph of IMF Strength in days for part (b). By looking through the data to find the data point at which day 118 starts and day 120 ends we found the range of the plot from data point 5399 to 21602.

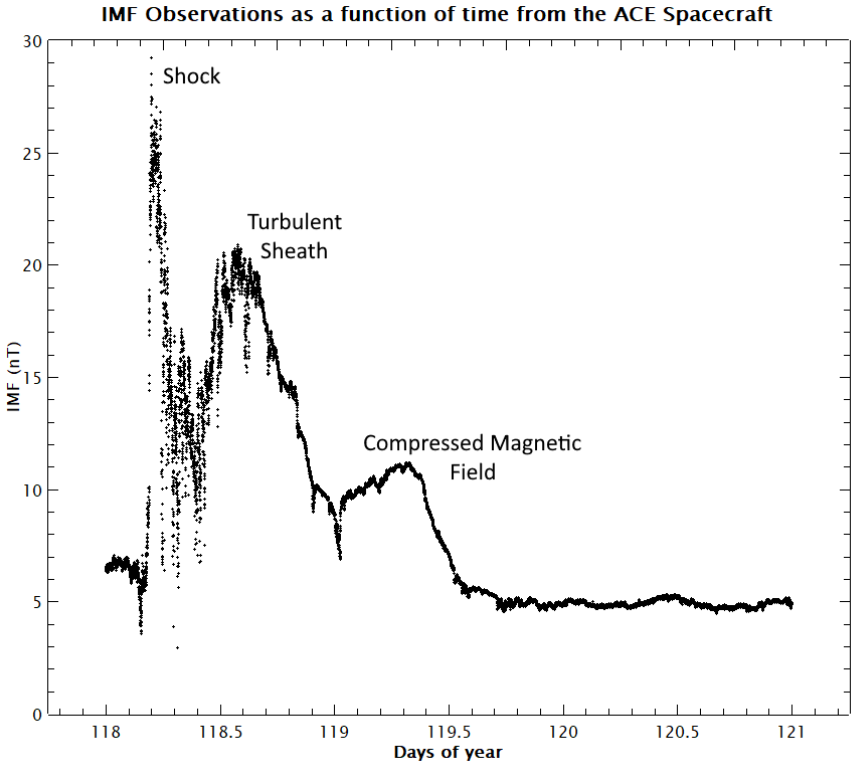

Figure 12: Graph of IMF strength as a function of time over the period of the ICME. This figure shows multipole peaks corresponding to the different parts of the ICME, the largest being the initial shock from the solar wind, the next being the turbulent sheath of the plasma and then the compressed magnetic field as the smallest peak before the IMF readings begin to normalise at approximately 5nT

16:19 There is a huge break in time as Overleaf servers went down so we changed focus to making sure we could continue and submit the lab book if the servers didn't come back up. We had issues since 13:00 which limited our ability to progress efficiently since we did not have a full offline backup.

Conclusion

16:36 Experiment 4: Solar Activity and the Solar Wind
In this experiment we explored the structure and dynamics of the IMF and the Solar Magnetosphere. We found that at Solar maxima, the Field Strength at north and south poles were equal and used this to deduce a solar cycle period of 11 years and the magnetic fields to have a period of 22 years demonstrating a complete cycle of the magnetic poles. Furthermore we found that the cause of the sunspots was due to the dynamic nature of the sun's magnetic field due to the cyclic nature of its poles. We then studied the IMF/Parker Spiral Magnetic Field and the distribution of directions, where we obtained that near-earth, the IMF generally points in 45° along the ecliptic, and 90°, corresponding to a near zero North-South component. This is consistent with the currently accepted values and expected results of the data analysis. Improvements we could make have made were to take more precise estimates and use more computational methods to help.